Biosensors and Bioelectronics 94 (2017) 651–656

Contents lists available at ScienceDirect

Biosensors and Bioelectronics

journal homepage: www.elsevier.com/locate/bios

A pH-responsive colorimetric strategy for DNA detection by acetylcholinesterase catalyzed hydrolysis and cascade amplification

Yuehua Guo, Kaili Yang, Jiachen Sun, Jie Wu, Huangxian Ju*

State Key Laboratory of Analytical Chemistry for Life Science, School of Chemistry and Chemical Engineering, Nanjing University, Nanjing 210023, PR China

ARTICLE INFO

Keywords:
Colorimetric strategy
pH-responsive
Acetylcholinesterase
Nonenzymatic cascade amplification
DNA detection

ABSTRACT

A pH-responsive colorimetric strategy was designed for sensitive and convenient biosensing by introducing acetylcholinesterase (AChE) catalyzed hydrolysis of acetylcholine to change solution pH and phenol red as an indicator. Using DNA as a target model, this technique was successfully employed for sensitive DNA analysis by labeling AChE to DNA. The sensitivity could be greatly improved by coupling a newly designed magnetic probe with target DNA-triggered nonenzymatic cascade amplification. In the presence of a help DNA (H) and the functional probe, the cascade assembly via toehold-mediated strand displacement released the AChE-conjugated sequence from magnetic beads, which could be simply separated from the reaction mixture to catalyze the hydrolysis of ACh in detection solution. The color change of detection solution from pink to orange-red, orange-yellow and ultimately yellow could be used for target DNA detection by naked eye and colorimetry with the absorbance ratio of detection solution at 558 nm to 432 nm as the signal. The nonenzymatically sensitized colorimetric strategy showed a linear range from 50 pM to 50 nM with a detection limit of 38 pM, indicating a promising application in DNA analysis.

1. Introduction

Colorimetric detection of nucleic acid with naked eye has received considerable attention due to its low cost, simplicity and practicality (Song et al., 2011; Zhou et al., 2014a). These colorimetric methods are generally performed through the aggregation of metal nanoparticles (Guo et al., 2013; Liu et al., 2013; Niazov-Elkan et al., 2014; Zagorovsky and Chan, 2013), and enzyme guided nanoparticles growth or etching (Guo et al., 2016; Yang et al., 2014) to change the color of detection solution. However, the aggregation is susceptible to high ionic strength or other impurities (Xia et al., 2010), which influences the reproducibility and detection precision, and thus limits their practical application. The enzyme-based nanoparticle colorimetric assay generally suffers the loss of enzyme activity and complex synthesis process of nanoparticles with specific morphologies (Guo et al., 2016; Yang et al., 2014). Thus enzyme mimics based colorimetric detection has been quickly developed (Chen et al., 2016a, 2016b; Kong et al., 2010; Park et al., 2011; Stefan et al., 2012; Tao et al., 2013; Zhang et al., 2011; Zhao et al., 2013). However, relatively low catalytic efficiency of these mimic enzymes leads to a lack of sensitivity. So, further improving the catalytic activity of nanozymes via surface modification is an interesting yet challenging task (Liu and Liu, 2017), and the design of novel colorimetric strategy with high sensitivity to circumvent the drawbacks for practical application is still an urgent demand.

The color change of detection solution can be conveniently achieved by adding pH-responsive dyes or pH indicators in the solution. Based on the monitoring of pH change, a variety of biosensors, logic gates, nanoreactors, nanodevices and even in vivo imaging methods have been developed (Grosso et al., 2015; Huang et al., 2014; Liu et al., 2007; Tram et al., 2014; Urano et al., 2009; Wang et al., 2015; Zhou et al., 2011) with fluorescent switch (Wang et al., 2015), nanoparticles (Zhou et al., 2011) or dye (Urano et al., 2009). The fluorescent switch can be designed through a pH gradient derived DNA i-motif folding to change the distance between fluorescent dye and quenching group for logical operations, enzyme activity assay and glucose sensing (Wang et al., 2015). A litmus-contained test solution has been proposed to monitor the pH change during the hydrolysis of urea catalyzed with urease for bacteria detection (Tram et al., 2014). Here acetylcholinesterase (AChE) catalyzed hydrolysis of acetylcholine (ACh) was designed as a novel strategy to regulate the pH of detection solution for colorimetric biosensing. Using phenol red as an indicator, this strategy could conveniently be developed for colorimetric biosensing of corresponding targets through conjugating AChE to different recognition

* Corresponding author.
E-mail address: hxju@nju.edu.cn (H. Ju).

http://dx.doi.org/10.1016/j.bios.2017.03.066
Received 22 January 2017; Received in revised form 28 March 2017; Accepted 30 March 2017
Available online 02 April 2017
0956-5663/

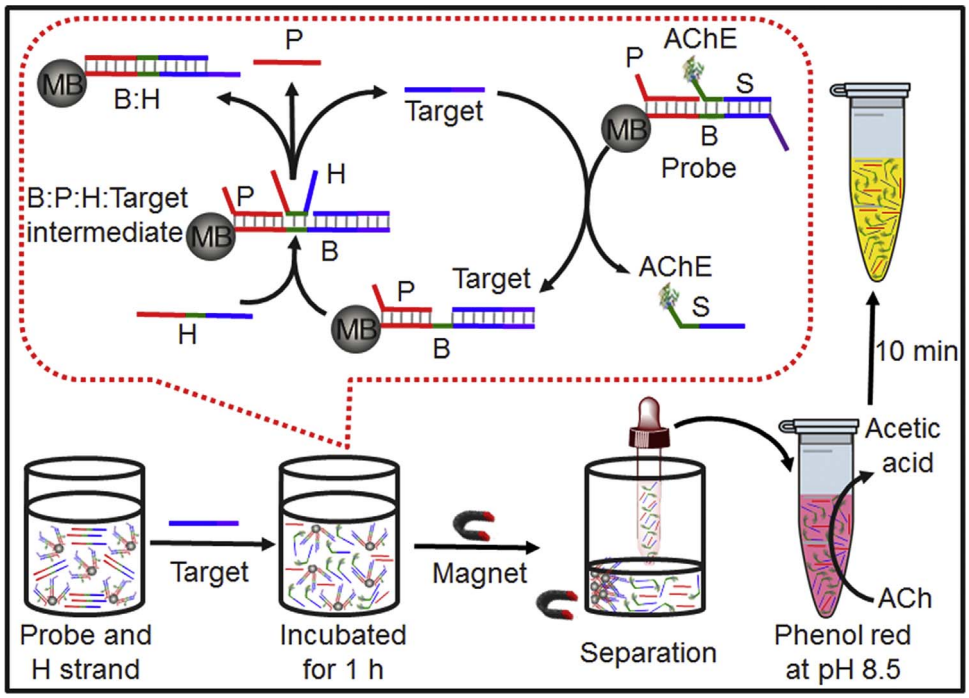

Fig. 1. Schematic diagram of the proposed pH-responsive colorimetric strategy for DNA detection sensitized with nonenzymatic cascade amplification.

elements. As proof of concept, a DNA sequence was conjugated with AChE to perform the DNA detection with naked eye and colorimetry. Furthermore, the AChE-conjugated DNA could be further introduced into a molecular programming to achieve nonenzymatic cascade amplification, which led to a highly sensitive colorimetric method for detection of target DNA (Fig. 1).

Recently, the nonenzymatic molecular programming, such as hybridization chain reaction (Dirks and Pierce, 2004; Huang et al., 2011), catalyzed hairpin assembly (Guo et al., 2015; Li et al., 2011, 2012; Yin et al., 2008), and entropy-driven catalysis (Lv et al., 2015; Wu et al., 2014; Zhang et al., 2007), is appealing for signal amplification. The entropy-driven catalysis can input specified sequence to catalyze the release of a specified oligonucleotide (Zhang et al., 2007), thus provides an amplifying circuit element for sensitive detection of DNA with fluorescent monitoring (Lv et al., 2015) and optical whispering gallery mode resonance (Wu et al., 2014). Here the entropy-driven catalytic system was further developed by introducing the AChE-conjugated DNA (S) to achieve a sensitized pH-responsive colorimetric detection. In this system, the recognition probe was prepared by immobilizing the hybridization product of biotin-labeled sequence B with S and an assistant sequence P on magnetic beads (MB) via streptavidin-biotin binding (Fig. 1). In the presence of a help sequence H, target DNA could act as an input sequence to catalyze the release of AChE-conjugated S via toehold-mediated strand displacement, which was then magnetically separated from the reaction mixture to catalyze the hydrolysis of ACh into acetic acid in detection solution. The decreasing pH led to a sensitive color change of phenol red for target DNA detection. The presented assay showed attractive features: (1) convenient signal readout using phenol red as the indicator, (2) high sensitivity due to the combination of AChE-mediated catalysis reaction with the entropy-driven catalytic system, (3) good expansibility for sensing biomolecules through labeling AChE to different recognition elements. Thus, the colorimetric strategy avoided the problems of previous strategies and showed a broad prospect in practical application.

2. Materials and methods

2.1. Materials and reagents

Streptavidin coated magnetic beads (1 μm in average diameter) were purchased from New England Biolabs (Ipswich, MA, USA). AChE, ACh, maleimidobenzoic acid N-hydroxy-succinimide ester (MBS), dimethyl sulphoxide (DMSO), tris(2-carboxyethyl)phosphine hydrochloride (TCEP), brilliant blue R, phenol red, and 4-(2-hydroxyethyl) piperazine-1-ethanesulfonic acid sodium (HEPES) were obtained from Sigma-Aldrich (St. Louis, MO, USA). Amicon centrifugal filters (10 kDa and 100 kDa molecular weight cutoff) were purchased from Millipore (Billerica, MA). The pH sensitive paper (special indicator paper 5.5–8.0) was purchased from Shanghai SSS Reagent Co., Ltd (China). Ultrapure water obtained from a Millipore water purification system (≥18 MΩ, Milli-Q, Millipore) was used in all assays. Phosphate buffer saline (PBS, 10 mM) was prepared by mixing the stock solutions of NaH_2PO_4 and Na_2HPO_4. The oligonucleotides were synthesized and purified using high performance liquid chromatography by Shanghai Sangon Biotechnology Co. Ltd. (China) and their sequences are listed in Table S1.

2.2. Apparatus

Polyacrylamide gel electrophoresis (PAGE) analysis was performed on an electrophoresis analyser (Bio-Rad, USA) and imaged on Bio-rad ChemDoc XRS (Bio-Rad, USA). The ultraviolet-visible (UV–vis) absorption spectra was carried out on a Synergy hybrid 1 multimode microplate reader (BioTek, USA) and nanodrop-2000C UV–vis spectrophotometer (Nanodrop, USA). A Mettler Toledo pH meter equipped with an InLab Ultra-Micro electrode from Mettler Toledo was used to monitor the pH changes.

2.3. Conjugation of AChE to DNA

Thiolated sequence S (1 mL, 100 μM) was firstly treated with 40 μL of 0.5 M TCEP in pH 5.5 10 mM PBS for 1 h, and the excess TCEP was removed with Millipore (10 kDa) for 8 times. For AChE conjugation,

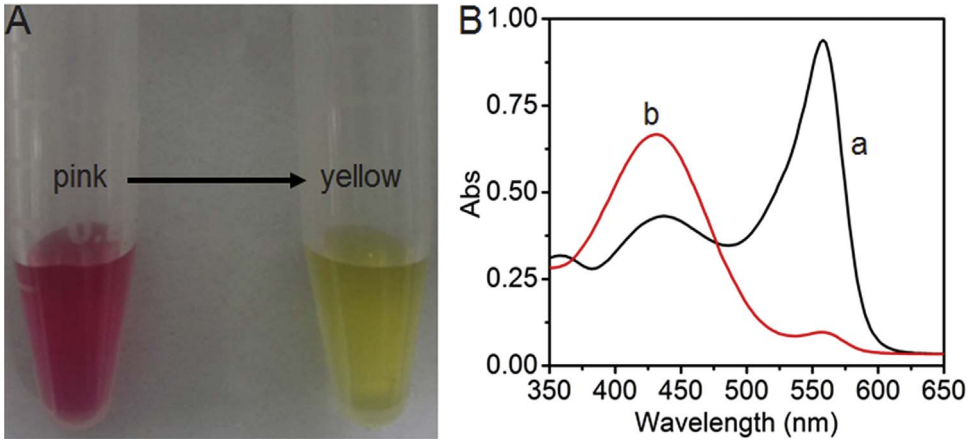

Fig. 2. (A) Colorimetric comparison and (B) UV absorption spectra of 150 μL of detection solutions in absence (pink, a) and presence (yellow, b) of 100 μL separated reaction product at 50 nM target DNA. The detection solution contained 150 mM NaCl, 10 mM ACh and 27 μg/mL phenol red in 0.1 mM pH 8.5 HEPES. (For interpretation of the references to color in this figure legend, the reader is referred to the web version of this article.)

1 mL of 1 mg/mL (4 μM) AChE was mixed with 25 μL DMSO solution of 6.4 mM MBS. After vortexing for 5 min, the solution was placed on a shaker for 1 h at room temperature, then the mixture was purified with Millipore (100 kDa) using pH 7.2 PBS for 8 times to remove excess MBS. After the MBS-activated AChE was reacted with treated thiolated S for 1 h, the product was purified with Millipore (100 kDa) using PBS for 8 times, and resuspended in 500 μL PBS.

2.4. PAGE and coomassie brilliant blue analysis

A 12% native polyacrylamide gel was prepared using 5×TBE buffer. The loading sample was the mixture of 7 μL target DNA, 1.5 μL 6×loading buffer, and 1.5 μL of UltraPowerTM dye. Before injection into the polyacrylamide hydrogel, the loading sample was placed for 3 min. The gel electrophoresis was run at 100 V for 1.5 h. The resulting board was illuminated with UV light and photographed with a Molecular Imager Gel Doc XR. After electrophoresis, the gel was stained for 1 h with 0.025% (w/v) coomassie brilliant blue R-250 dye prepared in staining solution containing methanol, distilled water and acetic acid at the ratios of 21:24:5, then destained for 5 h with a solution containing 5% methanol and 7% acetic acid.

2.5. Preparation of functional probe

1.25 mL of MB suspension (particle concentration: 4 mg/mL) was used for the preparation of the probe. MB was washed with 5 mL of 20 mM Tris-HCl containing 0.5 M NaCl (pH 8.0) three times and resuspended in 5 mL Tris-HCl, in which biotinylated B, P strand (500 μL, 10 μM, respectively) and AChE-DNA (500 μL, 8 μM) were added, followed by incubation with mild shaking at room temperature for 1 h. After removing the supernatant, the resulting probe was washed three times with 5 mL of 0.1 mM HEPES containing 150 mM NaCl (pH 8.5) and resuspended in 4 mL of HEPES.

2.6. Detection of target DNA

10 μL of target DNA solution or sample was mixed with 80 μL of probe and 10 μL of 10 μM H to incubated at room temperature for 1 h. After magnetic separation, 100 μL of the obtained mixture was added in 50 μL detection solution containing 150 mM NaCl, 10 mM ACh and 27 μg/mL phenol red to incubate at room temperature for 10 min. The obtained solution was used for colorimetric detection of target DNA.

3. Results and discussion

3.1. Feasibility of pH-responsive colorimetric strategy for DNA detection

The feasibility of pH-responsive colorimetric detection was firstly validated using AChE to replace the probe in a detection solution containing 150 mM NaCl, 10 mM ACh and 27 μg/mL phenol red (10 μL of 0.04% phenol red in 150 μL detection solution) in 0.1 mM pH 8.5 HEPES. The pH 8.5 detection solution showed two UV absorbance peaks at 558 nm and 432 nm, which are attributed to the deprotonated base form and the acid form of phenol red, respectively (Soller, 1994). Upon addition of AChE in the detection solution, its color changed from pink to yellow, while the absorbance peak at 558 nm decreased greatly and the absorbance peak at 432 nm increased (Fig. S1), indicating the decreasing base form and increasing acid form due to the change of pH from 8.5 to acidic pH with the following equation (Wang et al., 2015):

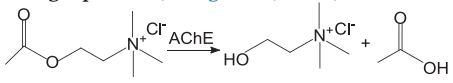

Thus the AChE catalytic reaction could be conveniently monitored with the color change or two absorbance peaks of phenol red. The concentration of phenol red in the detection solution for sensitive observation was optimized to be 27 μg/mL (Fig. S2), at which the color of the detection solution gradually changed from pink to orange-red, orange-yellow and ultimately yellow when the concentration of AChE increased from 0.3 to 8.0 nM (Fig. S3A). Thus the color was strongly dependent on the concentration of AChE. Moreover, the plot of absorbance ratio at 558 nm to 432 nm (A558/A432) vs the logarithm value of AChE concentration showed a good linearity (Fig. S3B), producing a method for detection of AChE concentration ranging from 0.3 to 6.7 nM with a detection limit of 190 pM (Fig. S3C).

After simply magnetic separation of the released AChE-conjugated S from the designed DNA assembly solution containing the functional probe, target DNA and help sequence H, the AChE-conjugated S could be added in the detection solution. The color and the absorbance peaks showed the same change as those shown in Fig. S1 (Fig. 2).

Thus the pH-responsive colorimetric strategy could be used for detection of target DNA through coupling with the target DNA triggered catalytic system for signal amplification.

3.2. Characterization of AChE-conjugated DNA

A bifunctional linker, MBS, was used to achieve the conjugation of AChE to thiolated sequence S (Fig. 3A). The AChE was first allowed to

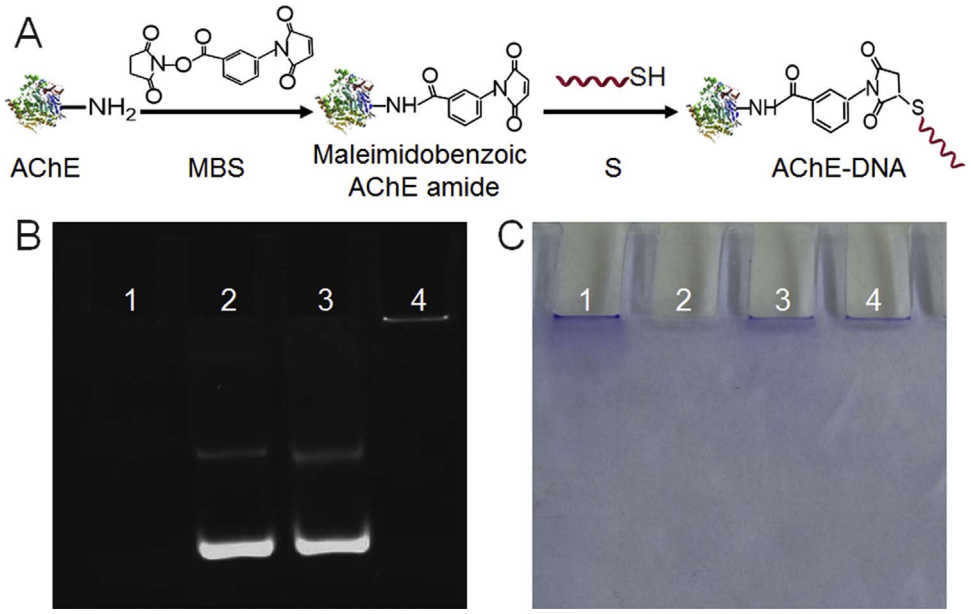

Fig. 3. (A) Illustration of the conjugation of AChE to sequence S. (B) Native PAGE and (C) protein-staining images. Lane 1: AChE (2 μM), lane 2: thiolated-S (50 μM), lane 3: mixture of thiolated-S (50 μM) and AChE (2 μM), lane 4: reaction product of S with AChE in presence of MBS after the removal of free DNA (2 μM).

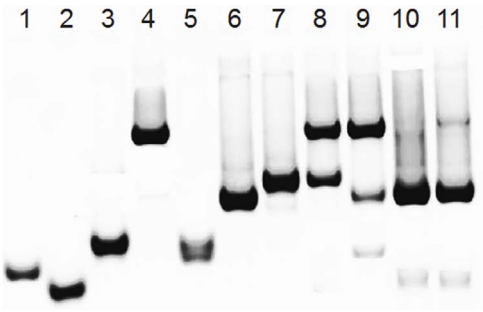

Fig. 4. PAGE analysis of nonenzymatic cascade amplification. Lane 1: S, lane 2: P, lane 3: B, lane 4: B:P:S complex, lane 5: H, lane 6: B:H duplex, lane 7: B:P:target complex, lane 8: mixture of B:P:S complex and target DNA, lane 9: mixture of B:P:S complex and H, lanes 10–11: mixture of B:P:S complex, H and target DNA. The concentrations of all sequences used in lanes 1–10 were 10 μM. The concentrations of B:P:S complex, H and target DNA in lane 11 were 10, 10 and 1 μM, respectively.

react with MBS to produce maleimidobenzoic AChE amide, which could then couple with –SH to form the AChE-DNA conjugate (Tram et al., 2014). PAGE and protein-staining images were used for the detection of DNA and AChE on the conjugate, respectively. As shown in Fig. 3B, thiolated sequence S and its mixture with AChE showed the bright band of S. The very weak band could be attributed to trace disulfide of thiolated S. After incubating the mixture with MBS linker, the band disappeared, and a new band of DNA occurred at the beginning position (lane 4), which could be attributed to the formation of the AChE-conjugated DNA. The large molecular weight of AChE (about 240 kDa) hindered the migration of the conjugate (Xiang and Lu, 2011). Moreover, the unreacted S and the trace disulfide could be efficiently removed from the conjugate by centrifugation. The protein-staining bands of AChE (lane 1), mixture of AChE and S (lane 3), and the conjugate (lane 4) showed very little difference (Fig. 3C), indicating the similar molecular weights of AChE (240 kDa) and the conjugate (about 280 kDa) (Xiang and Lu, 2011). For distinguishing AChE and AChE-DNA conjugate, SDS-PAGE experiment was conducted (Fig. S4). The AChE-DNA conjugate showed slower migration than AChE due to the larger molecular weight. These results demonstrated the successful conjugation of AChE to thiolated S.

The maximum absorption of the purified AChE-DNA conjugate occurred at 260 nm (Fig. S5), which was stronger than that of DNA at lower concentration, indicating more than one DNA on each AChE. The wider peak resulted from the absorption of AChE at 280 nm, which led to a mild shoulder at the spectrum (Zhou et al., 2014b). From the absorbances of DNA, AChE and AChE-DNA conjugate at both 260 and 280 nm, the molecular ratio of DNA versus AChE in the conjugate was calculated to be 4.2:1 (Zhou et al., 2014b).

3.3. Enzyme activity of AChE conjugated to S

The conjugation of DNA with AChE might affect the function or activity of the enzyme. Compared with the control, the color change of detection solution with the same AChE and AChE-DNA concentration did not show obvious difference (Fig. S6, inset), and their UV absorption spectra were almost identical (Fig. S6). Thus the activity of AChE could be almost completely retained.

3.4. Verification of nonenzymatic cascade amplification

To demonstrate the feasibility of the nonenzymatic cascade amplification, PAGE was carried out and showed in Fig. 4. Lanes 1–3 and 5 showed the bands of S, P, B and H, respectively, and the band of B:P:S complex could be observed in lane 4, which showed larger molecular weight than both B:H duplex and B:P:target complex (lanes 6 and 7) obtained by incubating B with H, and B, P with target DNA at room temperature for 1 h. After adding target DNA in the B:P:S complex, a new band was observed (lane 8), which was at the same position as the B:P:target complex, demonstrating that target DNA could displace S from the B:P:S complex to form B:P:target complex. After adding H in B:P:S complex, a weak band was observed at the same position as B:H duplex (lane 9), indicating the formation of B:H duplex with little amount. Upon addition of target DNA in the mixture of B:P:S complex and H, a new band was observed at the position of B:H duplex (lanes 10 and 11), while the band of B:P:S complex disappeared at both 10 and 1 μM target DNA (lanes 10 and 11), indicating the feasibility of the nonenzymatic cascade amplification.

3.5. Monitoring of pH change and DNA detection

The pH change of detection solution during the reaction process could be measured with pH paper strips. After 10 μL of the hydrolysis products obtained every two minutes from 150 μL detection solution

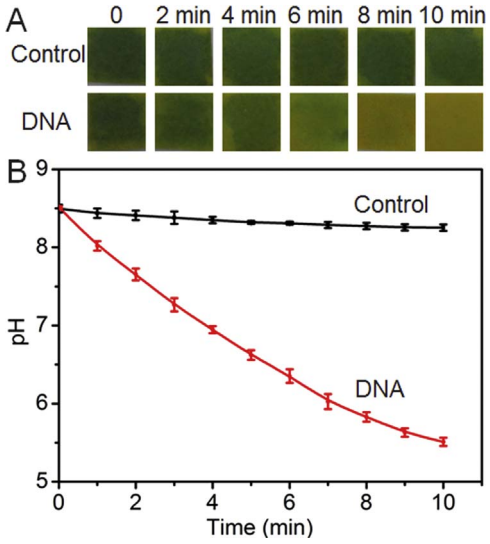

Fig. 5. (A) Monitoring pH changes every two minutes using pH paper strips and 10 μL of hydrolysis product, (B) plot pH of detection solution vs hydrolysis time. (For interpretation of the references to color in this figure, the reader is referred to the web version of this article.)

containing 100 μL of the magnetically separated AChE-DNA at 50 nM target DNA were added onto the pH paper strips, the color changed from blue to green-yellow, while the control sample kept blue (Fig. 5A), indicating the gradually decreasing pH of the detection solution, as monitored with a hand-held pH meter (Fig. 5B). The pH value of detection solution decreased nearly 3 pH units in 10 min.

For performing the detection of target DNA, the mixture of functional probe, help sequence H and target DNA was incubated at room temperature for 1 h, and then 100 μL of the separated AChE-DNA conjugate was used to catalyze the hydrolysis of ACh in detection solution. As expected, the color of detection solution gradually changed from pink to orange-red, orange-yellow and ultimately yellow when the concentration of target DNA increased from 50 pM to 100 nM (Fig. 6A). Meanwhile, their corresponding UV absorbance peaks at 432 and 558 nm gradually increased and decreased, respectively (Fig. 6B). The absorbance ratio at 558 to 432 nm was linearly proportional to the logarithm value of target DNA concentration over the range of 50 pM to 50 nM (Fig. 6C). The linear regression equation was A_{558}/A_{432} =−1.52 log [DNA] +2.45. Thus the detection limit at 3σ could be calculated to be 38 pM with the blank signals and the equation. Compared with some existing colorimetric DNA detection methods, this method provided wider concentration range and lower detection limit (Table S2). As control, the change of absorbance was examined at 50 nM target DNA in the absence and presence of help sequence H, and the latter showed greater change (Fig. S7), indicating that the strand displacement reaction amplified the detection signal. When the pH of detection solution was used as the signal, the corresponding method showed a detectable range of 50 pM to 100 nM for target DNA analysis (Fig. S8). To evaluate the practical application of the proposed strategy, recovery testing was carried out by spiking target DNA solution into 10% human serum. The spiked samples with 0.1 and 10 nM of target were measured, and the recoveries were 94% and 103%, respectively. The acceptable recoveries demonstrated the practical application of the proposed colorimetric strategy for DNA detection in real sample analysis.

The selectivity of the proposed pH-responsive colorimetric assay for DNA analysis was investigated by comparing the absorbance ratio at 558 to 432 nm with three different DNA sequences (Fig. S9). Compared with blank, the perfect complementary target showed the largest change of absorbance ratio, and single base-mismatched sequence led to a 37% decrease of absorbance ratio. The absorbance ratio for random DNA was closed to the blank solution. These results indicated that this colorimetric assay possessed excellent capability to differentiate perfectly matched and mismatched DNA, demonstrating the excellent selectivity of this method.

4. Conclusions

The work proposes a method to regulate the pH of detection solution by using AChE catalyzed hydrolysis of ACh to produce acetic acid for colorimetric or visual detection of biomolecules with phenol red as an indicator. The color of the detection solution shows a wide and continuous change with the increasing concentration of AChE. This technique has successfully been employed for sensitive DNA analysis by introduction of nonenzymatic cascade signal amplification with a newly designed probe and target triggered DNA assembly. With the absorbance ratio of detection solution at 558 nm to 432 nm as the signal, this method shows a wide detectable concentration range and

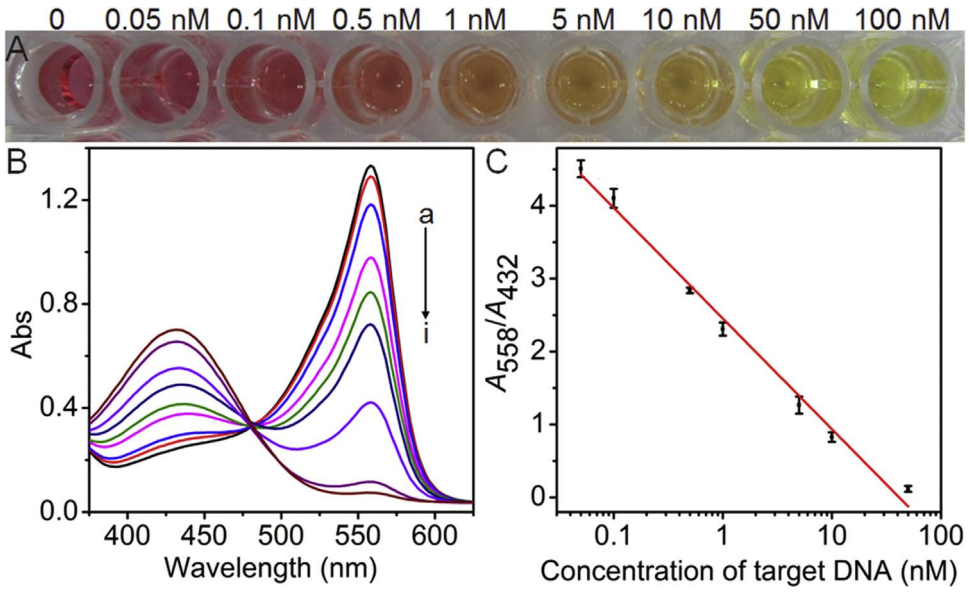

Fig. 6. (A) Photograph of detection solutions containing 100 μL of the separated product at marked concentration of target DNA for 10 min, (B) UV–vis spectra of detection solutions at 0, 0.05, 0.1, 0.5, 1, 5, 10, 50, 100 nM target DNA (from a to i), (C) plot of absorption ratio at 558 nm to 432 nm vs logarithm of DNA concentration. (For interpretation of the references to color in this figure, the reader is referred to the web version of this article.)

high sensitivity. Through labeling AChE to different recognition elements, this strategy can be extended for colorimetric biosensing of different targets. The convenient operation with magnetic separation, rapid detection, and excellent performance shows a broad prospect of this strategy in practical application.

Acknowledgments

We gratefully acknowledge the National Natural Science Foundation of China (21135002, 21121091, and 21361162002), Program for New Century Excellent Talents in University of Ministry of Education of China (NCET-13-0283) and Priority development areas of The National Research Foundation for the Doctoral Program of Higher Education of China (20130091130005).

Appendix A. Supporting information

Supplementary information associated with this article can be found in the online version at doi:10.1016/j.bios.2017.03.066.

References

Chen, J., Ge, J., Zhang, L., Li, Z.H., Li, J.J., Sun, Y.J., Qu, L.B., 2016a. Microchim. Acta 183, 1847–1853.
Chen, J., Ge, J., Zhang, L., Li, Z.H., Qu, L.B., 2016b. Sens. Actuators B: Chem. 233, 438–444.
Dirks, R.M., Pierce, N.A., 2004. Proc. Natl. Acad. Sci. USA 101, 15275–15278.
Grosso, E.D., Dallaire, A.M., Vallée-Bélisle, A., Ricci, F., 2015. Nano Lett. 15, 8407–8411.
Guo, L.H., Xu, Y., Ferhan, A.R., Chen, G.N., Kim, D.H., 2013. J. Am. Chem. Soc. 135, 12338–12345.
Guo, Y.H., Wu, J., Ju, H.X., 2015. Chem. Sci. 6, 4318–4323.
Guo, Y.H., Wu, J., Li, J., Ju, H.X., 2016. Biosens. Bioelectron. 78, 267–273.
Huang, J., Wu, Y.R., Chen, Y., Zhu, Z., Yang, X.H., Yang, C.Y.J., Wang, K.M., Tan, W.H., 2011. Angew. Chem. Int. Ed. 50, 401–404.
Huang, Y.Y., Lin, Y.H., Ran, X., Ren, J.S., Qu, X.G., 2014. Nanoscale 6, 11328–11335.
Kong, D.M., Xu, J., Shen, H.X., 2010. Anal. Chem. 82, 6148–6153.
Li, B.L., Ellington, A.D., Chen, X., 2011. Nucleic Acids Res. 39, e110.
Li, B.L., Jiang, Y., Chen, X., Ellington, A.D., 2012. J. Am. Chem. Soc. 134, 13918–13921.
Liu, B.W., Liu, J.W., 2017. Nano Res.. http://dx.doi.org/10.1007/s12274-017-1426-5.
Liu, H.J., Xu, Y., Li, F.Y., Yang, Y., Wang, W.X., Song, Y.L., Liu, D.S., 2007. Angew. Chem. Int. Ed. 46, 2515–2517.
Liu, P., Yang, X.H., Sun, S., Wang, Q., Wang, K.M., Huang, J., Liu, J.B., He, L.L., 2013. Anal. Chem. 85, 7689–7695.
Lv, Y.F., Cui, L., Peng, R.Z., Zhao, Z.L., Qiu, L.P., Chen, H.P., Jin, C., Zhang, X.B., Tan, W.H., 2015. Anal. Chem. 87, 11714–11720.
Niazov-Elkan, A., Golub, E., Sharon, E., Balogh, D., Willner, I., 2014. Small 10, 2883–2891.
Park, K.S., Kim, M.I., Cho, D.Y., Park, H.G., 2011. Small 7, 1521–1525.
Soller, B.R., 1994. IEEE Eng. Med. Biol. 13, 327–335.
Song, Y.J., Wei, W.L., Qu, X.G., 2011. Adv. Mater. 23, 4215–4236.
Stefan, L., Denat, F., Monchaud, D., 2012. Nucleic Acids Res. 40, 8759–8772.
Tao, Y., Lin, Y.H., Ren, J.S., Qu, X.G., 2013. Biomaterials 34, 4810–4817.
Tram, K., Kanda, P., Salena, B.J., Huan, S.Y., Li, Y.F., 2014. Angew. Chem. Int. Ed. 53, 12799–12802.
Urano, Y., Asanuma, D., Hama, Y., Koyama, Y., Barrett, T., Kamiya, M., Nagano, T., Watanabe, T., Hasegawa, A., Choyke, P.L., Kobayashi, H., 2009. Nat. Med. 15, 104–109.
Wang, M., Zhang, G.X., Zhang, D.Q., 2015. Chem. Commun. 51, 3812–3815.
Wu, Y.Q., Zhang, D.Y., Yin, P., Vollmer, F., 2014. Small 10, 2067–2076.
Xia, F., Zuo, X.L., Yang, R.Q., Xiao, Y., Kang, D., Vallée-Bélisleb, A., Gong, X., Yuen, J.D., Hsu, B.B.Y., Heeger, A.J., Plaxco, K.W., 2010. Proc. Natl. Acad. Sci. USA 107, 10837–10841.
Xiang, Y., Lu, Y., 2011. Nat. Chem. 3, 697–703.
Yang, X.J., Yu, Y.B., Gao, Z.Q., 2014. ACS Nano 8, 4902–4907.
Yin, P., Choi, H.M.T., Calvert, C.R., Pierce, N.A., 2008. Nature 451, 318–323.
Zagorovsky, K., Chan, W.C.W., 2013. Angew. Chem. Int. Ed. 52, 3168–3171.
Zhang, D.Y., Turberfield, A.J., Yurke, B., Winfree, E., 2007. Science 318, 1121–1125.
Zhang, L.B., Zhu, J.B., Li, T., Wang, E.K., 2011. Anal. Chem. 83, 8871–8876.
Zhao, Y.Y., Zhou, L., Tang, Z., 2013. Nat. Commun. 4, 1493–1500.
Zhou, C.H., Zhao, J.Y., Pang, D.W., Zhang, Z.L., 2014a. Anal. Chem. 86, 2752–2759.
Zhou, K., Wang, Y., Huang, X., Luby-Phelps, K., Sumer, B.D., Gao, J., 2011. Angew. Chem. Int. Ed. 50, 6109–6114.
Zhou, Z.J., Xiang, Y., Tong, A.J., Lu, Y., 2014b. Anal. Chem. 86, 3869–3875.